

Charge-stabilized colloidal suspensions. Phase behavior and effects of confinement*

R. Klein and H. H. von Grünberg

Fachbereich Physik, Universität Konstanz, 78457 Konstanz, Germany

Abstract: The Poisson–Boltzmann (PB) equation is used to investigate effective colloid–interface interactions and the phase behavior of charge-stabilized colloidal suspensions. When a colloidal particle, immersed in an electrolyte, approaches an interface, which may be neutral (such as air) or charged (like electrodes, glass, etc.), image charge effects plus the deformation of the colloidal ion atmosphere by the interface lead to an effective interaction which can be attractive or repulsive, depending on the surface charge density and the dielectric constants of the interface and the electrolyte. Two cases are considered: i) a spherical particle near a like-charged interface, and ii) a rod-like particle in the vicinity of an oppositely charged interface. The latter serves as a model for the adsorption of (anionic) DNA on a cationic membrane, and it is shown that the effective attraction, induced by the release of counterions on approach of the DNA to the membrane, makes up an essential contribution to the total DNA–membrane effective interaction. To understand the phase behavior of charge-stabilized colloidal suspensions, we study a PB cell model of a bulk suspension and investigate how the PB equation can best be linearized. It is found that the previously predicted gas–liquid phase coexistence results when the PB equation is linearized about the Donnan potential. No indication of such a spinodal instability could, however, be found, when the free energy is evaluated using the numerical solution of the full PB equation. This suggests that the predicted gas–liquid phase coexistence is an artifact of the linearization.

INTRODUCTION

When a colloidal particle carrying ionizable groups at its surface is suspended in a polar solvent, dissociation of the surface groups sets in, leading to a net charge of the colloidal surface. The oppositely charged dissociated small ions, the counterions, surround the colloidal particle and form the electric double layer. The thickness of this layer is determined by two competing effects: thermal motion tends to spread the layer, thereby increasing the contribution of the small ions to the total entropy, while the electrostatic attraction between the counterions and the colloidal surface works in quite the opposite direction. In many cases, the suspending fluid contains additional salt, which provides further counterions but also coions having the same sign of charge as the colloid.

There are many colloidal particles of this kind having scientific or technological significance. Polystyrene spheres, for example, may carry several thousands of elementary charges on their surface, being surrounded by a correspondingly large number of counterions. Ionic micelles and proteins carry much fewer charges, but their character as charged particles is important to understand their structure and dynamics. Many biomolecules are polyelectrolytes, among them such most prominent examples as DNA, in aqueous solutions a highly charged polymer.

*Plenary lecture presented at the 27th International Conference on Solution Chemistry, Vaals, The Netherlands, 26–31 August 2001. Other presentations are published in this issue, pp. 1679–1748.

Details of the distribution of small ions around colloidal particles are important to understand the interaction between them or their interaction with charged or uncharged geometric confinements, such as the interface between the electrolyte solution containing the colloids and another material like air or glass or a membrane. Despite the long history of colloid science, this is still an active area of research [1,2]. It has become clear now that the celebrated Derjaguin–Landau–Verwey–Overbeek (DLVO) theory [3] has its limitations. An obvious case is the presence of interfaces or boundaries, where the confinement of the electrical double layer gives rise to a nonspherical distribution of the ions already for neutral walls. Usually, the dielectric properties of the wall material are quite different from those of the solvent, which is here taken to be water, so that image charge effects inevitably arise. They can have significant effects on the colloid-wall interaction at small distances, even when the wall is charged.

The electrostatic contribution to the DLVO potential between like-charged objects is repulsive. It is an effective, state-dependent interaction, which is obtained by tracing-out (coarse-graining) the small ions, which necessarily has to be done by some approximate procedures (e.g., mean-field approximation). Another contribution to the total free energy, which goes beyond mean-field, arises from correlations between the small ions, but this is difficult to treat properly. Ever since it was first discovered that correlations between divalent counterions may result in an effective attraction between like-charged planar double layers [4], the importance of small-ion correlations has been established many times and by several different approaches [1,2,5]. Although these correlations are not completely negligible for monovalent counterions, attraction is observed only with divalent ones. In this contribution, considerations will be limited to the case of monovalent ions, so our mean-field treatment can be expected to deliver qualitatively correct results.

Under these circumstances, the ion distribution around charged objects is governed by the nonlinear PB equation, and our objective here is to investigate the consequences of the nonlinear character of this equation in various situations. One of them is the interaction of a spherical particle or a rod-like particle with a charged or neutral interface. How do these particles, immersed in an aqueous electrolyte solution, interact with a material having dielectric properties very different from those of water and having a surface charge density either equal or opposite in sign from the charge on the particle? These investigations are related to recent experiments. In a first one, total internal reflection microscopy (TIRM) is used to measure the interaction potential between a colloidal particle and a charged dielectric wall [6]. A second case is related to several experiments where the behavior of (negatively charged) DNA in the vicinity of a cationic membrane is investigated [7].

Finally, the nonlinear PB equation is also very useful to study concentrated colloid suspensions in bulk. The interest in this case arises from the interesting phase behavior of charge-stabilized suspensions. If their thermodynamic properties could be fully understood on the basis of pair-wise-additive repulsive DLVO potentials, the suspension should not exhibit a fluid–fluid critical point, since the coexistence of a colloid-rich, liquid-like phase with a colloid-poor, gas-like phase requires necessarily attractive interactions. A number of experiments on highly de-ionized suspensions [8], however, suggest that this kind of coexistence nevertheless exists, a remarkable fact which can have two explanations: either the effective pair-potential is not DLVO-like and repulsive at large distances, but in fact attractive, or, the assumption of pair-wise additivity breaks down and more than a simple summation of pair-potentials is needed to approximate the total free energy of the suspension. In the final part of this paper, the present status of our understanding of this intriguing problem will be briefly discussed.

CHARGED SPHERICAL COLLOID INTERACTING WITH A LIKE-CHARGED PLANAR INTERFACE

Concept of effective interactions

A colloidal particle of radius a , carrying Z negative elementary charges e on its surface has a distance h of its center to a planar wall having a surface charge density: $-e\sigma_w$. The particle is immersed in a 1:1

electrolyte occupying the half-space $z > 0$. The distributions $\rho_{\pm}(\mathbf{r})$ of positive and negative small ions are related to the dimensionless electrostatic potential $\phi(\mathbf{r}) = \beta e \psi(\mathbf{r})$ by $\rho_{\pm} = c_s e^{\mp \phi}$, where ψ denotes the electrostatic potential, $\beta = 1/k_B T$ and c_s the bulk concentration of positive and negative micro-ions, far away from the interface and the colloid particle. The potential $\phi(\mathbf{r})$ satisfies the PB equation for $z \geq 0$ (but outside the colloid) and the Laplace equation for $z < 0$,

$$\nabla^2 \phi(\mathbf{r}) = \kappa^2 \sinh \phi(\mathbf{r}) ; \quad z \geq 0 \quad (1)$$

$$\nabla^2 \phi(\mathbf{r}) = 0 ; \quad z < 0 \quad (2)$$

where $\kappa^2 = 8\pi\lambda_B c_s$ defines the screening parameter with $\lambda_B = e^2 \beta / \epsilon$ being the Bjerrum length and ϵ the dielectric constant of the solvent ($\epsilon \approx 78$; $\lambda_B \approx 0.7$ nm for water). The surface charges on wall and particle enter the problem through the boundary conditions; the geometry of the problem is shown in Fig. 1.

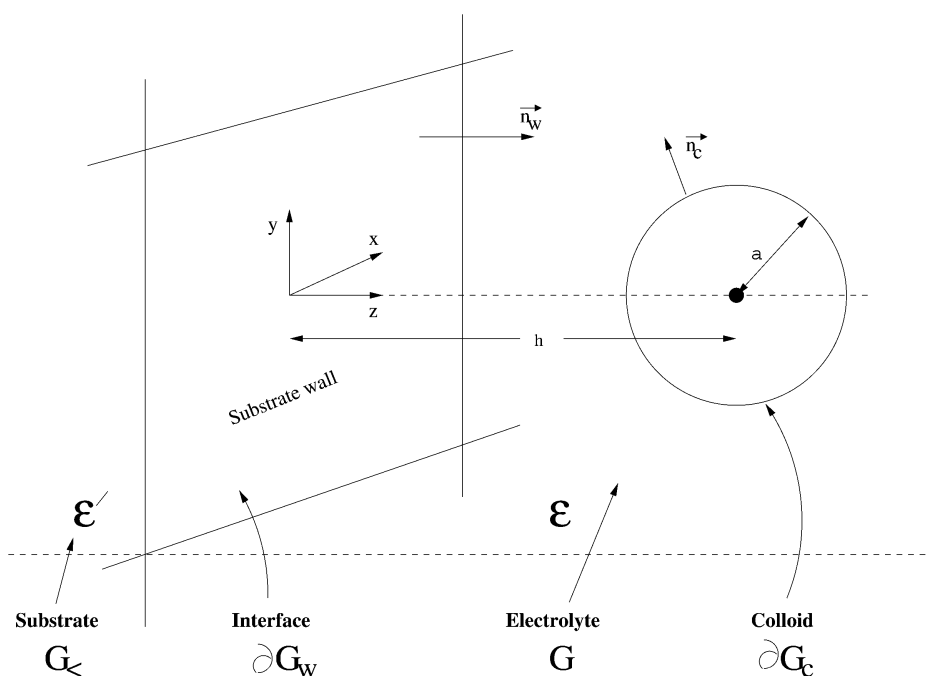


Fig. 1 Our system: a colloid of charge $-Ze$ and radius a inside an electrolytic solution of dielectric constant ϵ , a distance h away from a substrate of dielectric constant ϵ' .

Denoting the surface charge density on the colloid by $\sigma_c = Z / 4\pi a^2$ and assuming constant-charge boundary conditions, one has

$$\mathbf{n}_c \cdot \nabla \phi(\mathbf{r}) = 4\pi\lambda_B \sigma_c \quad (3)$$

for \mathbf{r} on the surface of the colloid ∂G_c ; \mathbf{n}_c is the outward normal unit vector (see Fig. 1). For the interface,

$$\epsilon \frac{\partial \phi}{\partial z} \Big|_{z=0^+} - \epsilon' \frac{\partial \phi}{\partial z} \Big|_{z=0^-} = 4\pi\lambda_B \sigma_w, \quad (4)$$

where ϵ' is the dielectric constant of the material at $z < 0$.

Equations 1 to 4 constitute the boundary value problem which has to be solved to obtain $\phi(\mathbf{r})$ and the nonuniform ion distribution $\rho_{\pm}(\mathbf{r})$. Once these quantities are known the effective interaction potential between the particle and the interface can be obtained from the grand canonical potential $\Omega(V, T, \mu_s)$,

$$\beta\Omega = \frac{1}{8\pi\lambda_B} \int_G d\mathbf{r} (\nabla\phi)^2 + \frac{\epsilon'}{8\pi\lambda_B\epsilon} \int_{G_{<}} d\mathbf{r} (\nabla\phi)^2 + \sum_{\alpha=\pm} \int_G d\mathbf{r} \rho_{\alpha} (\log \rho_{\alpha} \Lambda^3 - 1) - \int_G d\mathbf{r} [\beta\mu_s (\rho_+ + \rho_-) - 2c_s] - \beta W^{SE}. \quad (5)$$

The first two terms describe the energy stored in the electric fields in regions G and $G_{<}$, where G is the half-space $z > 0$ without the region occupied by the colloidal particle and $G_{<}$ is the half-space $z < 0$ having the dielectric constant ϵ' . The third term is the entropy of mixing of the small ions, with Λ the de Broglie wavelength; the fourth term takes care of the nonuniform spatial distribution of the small ions, where the chemical potential μ_s is related to the equilibrium concentration c_s of ions by $\beta\mu_s = \log c_s \Lambda^3$. The last term is a constant which is convenient for calculational reasons; it is the (self) energy of a charged, unscreened, and isolated colloid in its own Coulomb field, $Z^2\lambda_B/2a$. Equation 5 can be rewritten by using eqs. 1 to 4 and Green's identity as

$$\beta\Omega_h = -\frac{\sigma_w}{2} \int_{\partial G_w} dS \phi_h - \frac{\sigma_c}{2} \int_{\partial G_c} dS \phi_h + c_s \int_G d\mathbf{r} [\phi_h \sinh \phi_h - 2 \cosh \phi_h + 2] - \beta W^{SE}. \quad (6)$$

The first term is the surface integral extended over the interface ∂G_w and the second one over the surface of the colloid ∂G_c . The index h is a reminder that ϕ_h is the solution of the boundary value problem in which the colloid-interface distance is fixed to h . The effective interaction of the colloid with the interface is then given by the change of the grand canonical potential when the colloid is brought from $h = \infty$ to the finite distance h ,

$$\beta V(h) = \beta(\Omega_h - \Omega_{\infty}). \quad (7)$$

$V(h)$ can now be obtained by solving eqs. 1–4 for many values of h and evaluating the integrals in eq. 6. Once Ω_h is known, other thermodynamic quantities like the number of small ions N involved in the screening of wall and particle charges, the internal energy U , the entropy S , etc. can be calculated by taking the appropriate derivatives.

Our PB boundary value problem cannot be solved analytically. It is, nevertheless, an instructive exercise to construct closed approximative expressions, as they best illustrate the content of the underlying physics. Moreover, they are useful in analyzing experiments, if their range of validity is tested against the exact solution [9].

Case of a neutral interface

Let us begin with the case of a neutral interface ($\sigma_w = 0$), for which the solution of the linearized PB equation for a point-like colloidal charge $-Ze$ immersed in an electrolyte is known [10],

$$\phi_h^{St}(s, z) = -Z\lambda_B\kappa \int_0^{\infty} dl J_0(\kappa sl) \frac{l}{\tilde{l}} \left[e^{-\kappa|z-h|\tilde{l}} + \chi(l) e^{-\kappa(z+h)\tilde{l}} \right]. \quad (8)$$

Here, $s^2 = x^2 + y^2$ and $\tilde{l}^2 = 1 + l^2$. The quantity $\chi(l)$ is given by

$$\chi(l) = \frac{\alpha(\tilde{l} + l) - 1}{\alpha(\tilde{l} - l) + 1} \quad (9)$$

where $\alpha = \epsilon / (\epsilon + \epsilon')$. This parameter approaches 1 for $\epsilon \gg \epsilon'$, which is the case when an aqueous electrolyte is in contact with dielectrics such as air, glass, and biologically relevant material, all of which

have a relatively small dielectric constant compared to water. In the opposite case, $\epsilon \ll \epsilon'$, the parameter α goes to zero, a case realized, for example, by a metal surface. The physical content of the result in eq. 8 becomes clear in the limit of vanishing electrolyte concentration, $c_s \rightarrow 0$, where

$$\phi_h^{St}(s, z) \rightarrow -Z\lambda_B \left[\frac{1}{|\mathbf{r} - h\mathbf{e}_z|} + \frac{2\alpha - 1}{|\mathbf{r} + h\mathbf{e}_z|} \right]. \quad (10)$$

This is the sum of the Coulomb potential of the test point charge at $z = h$ and of another point charge (the image charge) at $z = -h$. Since $2\alpha - 1 = 1$ for $\epsilon \gg \epsilon'$, the point test charge is repelled from an uncharged glass or air interface, whereas $2\alpha - 1 = -1$ for $\epsilon \ll \epsilon'$, so that it is attracted to a metal surface.

Expression 8 can now be used in eqs. 7 and 6, which simplifies in linear theory because the integrand of the third term in eq. 6 is of the order of ϕ^2 and can therefore be neglected. The result for the effective colloid-wall potential then is [9]

$$\beta V^{St}(h) = \frac{Z^2 \lambda_B \kappa}{2} \int_0^l dl \frac{l}{\tilde{l}} \chi(l) e^{-2\kappa h \tilde{l}}. \quad (11)$$

This expression further simplifies in the limit $\alpha = 1$ and $\alpha = 0$, where

$$\beta V^{St}(h) = \pm \frac{1}{2} Z^2 \lambda_B \kappa \frac{e^{-2\kappa h}}{2\kappa h} \quad (12)$$

is obtained; the upper (lower) sign applies to $\alpha = 1$ ($\alpha = 0$). This result is easy to understand. Without electrolyte ($\kappa = 0$), the point charge at h sees a potential $\pm Z\lambda_B/2h$, and the wall-colloid interaction potential is $\pm Z^2\lambda_B/4h$. The presence of an electrolyte ($\kappa > 0$) introduces screening, which leads to the familiar exponential factor $e^{-2\kappa h}$ in eq. 12. When the interface has the same dielectric constant as the solvent ($\epsilon' = \epsilon$) which corresponds to $\alpha = 1/2$, there is no image charge effect, but eq. 11 gives $\beta V^{St}(h) > 0$ [9]. There is still repulsion from the interface, which arises from the distortion of the screening cloud of small ions due to the geometrical confinement.

One of the major assumptions in the derivation of the Stillinger potential, eq. 8, is the point-like character of the colloidal particle. The error thus introduced can subsequently be corrected by charge-renormalization. The main error in using eq. 11 for the interaction of an interface with a colloid of finite radius a arises from the fact that one allows counter- and coions to access the space inside the sphere of radius a where, in reality, they are excluded from. This sphere, therefore, contains the charge

$$gZ \equiv Z - 4\pi \int_0^a dr r^2 [\rho_+(r) - \rho_-(r)] = Ze^{-\kappa a} (1 + \kappa a) \quad (13)$$

where for simplicity $\rho_{\pm}(r)$ are taken to be the Debye-Hückel ionic charge densities around the colloidal point charge in bulk [$\rho_+(r) - \rho_-(r) = Z\kappa^2 \exp(-\kappa r)/(4\pi r)$]. Since $g < 1$, the spherical region around the test charge contains less than Z charges. In order that the ions outside this sphere see the charge Z , corresponding to a colloidal particle of radius a , the value of the point test charge has to be increased to $Z^* = Z/g = Ze^{\kappa a}/(1 + \kappa a)$. The result for g in eq. 13 applies to $h \rightarrow \infty$, since it assumes spherical symmetry for $\rho_{\pm}(r)$. It has been shown [9] that the correction due to the finite distance h from the interface, which takes care of the asymmetric ion distributions, is less than a few percent. Therefore, it is sufficient to use the value for the renormalized charge, which is found in bulk, also for the particle in the vicinity of an interface.

For the case $\epsilon \gg \epsilon'$ the effective colloid-interface potential is now obtained from eq. 12 by replacing Z by Z^* ,

$$\beta V^{St}(h) = \frac{Z^2 \lambda_B}{2(1 + \kappa a)^2} \frac{e^{-2\kappa(h-a)}}{2h}. \quad (14)$$

The validity of this approximate result has been tested by comparing with the numerical solution of the PB equation [9]. It is found that eq. 14 is within 10% error as long as the surface potential on the colloid $\Phi_c \leq 1$ and $\kappa(h-a) > 0.6$. The relation between the colloid charge Z and Φ_c is $Z = (2\kappa a^2/\lambda_B) |\sinh \Phi_c/2|$. The value $\Phi_c = 1$ marks the limit of linear theory which is the other major assumption made in deriving the Stillinger potential. It is, therefore, not surprising that eq. 14 ceases to give good results when $\Phi_c > 1$.

Charged interface

The PB boundary value problem has been solved analytically for a charged planar wall in the absence of a colloid by Gouy and Chapman [11]

$$\Phi^{GC}(z) = 4\text{arctanh}(e^{-\kappa z} \tanh(\Phi_w/4)) \quad (15)$$

where the potential at the wall Φ_w is related to the surface charge density by

$$4\pi\lambda_B\sigma_w = -2\kappa \sinh(\Phi_w/2). \quad (16)$$

When $\kappa z > 1$ eq. 15 can be approximated by

$$\phi^{GC}(z) = -4\gamma_w e^{-\kappa z} \quad (17)$$

with $\gamma_w = |\tanh(\Phi_w/4)|$. Placing the colloidal surface charge density $\sigma_c = Z/4\pi a^2$ into this potential and appropriately renormalizing the charge to take care of the finite size of the colloid, the Gouy–Chapman potential can also be used as an approximation of the potential around the colloidal particle. Superposing both potentials and evaluating eqs. 6 and 7 the following expression for the electrostatic interaction potential can be derived [9]

$$\beta V(h) = \frac{16a\gamma_c\gamma_w}{\lambda_B} e^{-\kappa(h-a)}, \quad (18)$$

where γ_c is related to σ_c just as γ_w is to σ_w .

Having the two approximate results, eq. 14 for the neutral interface, describing the image charge effects and the distortion of the small ion distributions, and eq. 18 for the direct electrostatic interaction between the charged interface and the colloid, it is not *a priori* clear whether adding the two gives a reasonable approximation for the total wall-colloid interaction. This problem arises from the nonlinear character of the PB equation, which in principle forbids the superposition of potentials. It is, therefore, essential to test the approximate potentials by comparing with the full numerical solution (i.e., solution of eqs. 1–4 inserted into eqs. 6 and 7) for the set of parameters κa , κh , Φ_w , and Φ_c . Extensive tests of this kind for this and various other constructed interaction potentials have been performed [9], and Fig. 2 gives an example of these results for the effective interaction potential in eq. 18 based on the Gouy–Chapman solution. The figure displays regions in the plane, spanned by the parameters κa and $\kappa(h-a)$, in which eq. 18 deviates less than 10% from the full solution to the PB problem. It is found that eq. 18 is an acceptable approximation provided that κa is sufficiently large. Increasing Φ_c while keeping Φ_w constant enlarges the region with an error below 10%.

Experiment measuring the colloid-wall potential

One of several experimental methods to determine the effective colloid-wall potential is total internal reflection microscopy (TIRM) [12]. The colloid particle with its center having a distance h from a horizontal glass plate experiences the gravitational potential $G_{eff}(h-a)$ and a van der Waals dispersion potential, which both attract it to the glass plate. The particle is prevented from adsorption by the repul-

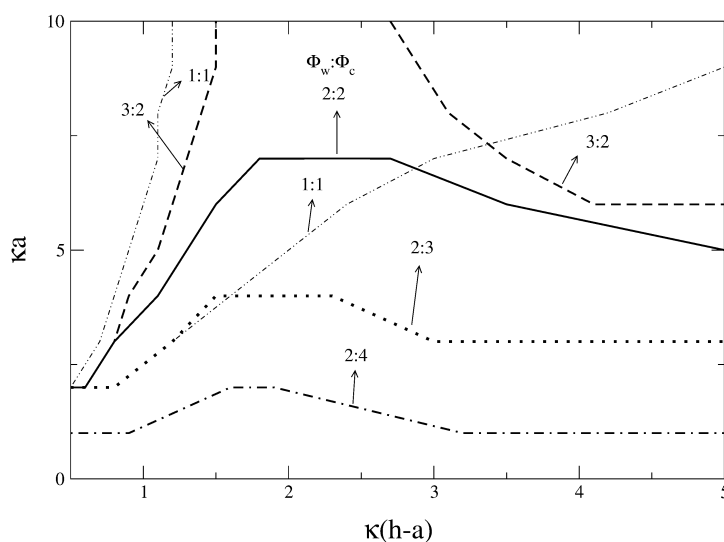


Fig. 2 An error contour diagram for the approximate potential in eq. 18 for various combinations of Φ_w and Φ_c . The arrows point to that part of the $[\kappa a, \kappa(h-a)]$ -plane where the error is less than 10% when compared to the exact numerical solution of the full PB problem. Taken from [9].

sive effects that we have just discussed. Except at very small distances, the dispersion force contribution is negligible, so the total potential is

$$V_{total}(h) = G_{eff}(h-a) + V(h), \quad (19)$$

where the effective gravitational constant is $G_{eff} = (4\pi a^3/3)g(\rho_c - \rho_w)$ with ρ_c and ρ_w denoting the mass densities of colloid and water, respectively, and g the gravitational constant. The potential $V_{total}(h)$ has a minimum at a value h_m ; it rises essentially linearly with h for $h > h_m$ due to the gravitational part and exponentially for $h < h_m$ because of the double-layer repulsion. Within this potential the particle executes Brownian motion.

The potential $V_{total}(h)$ is experimentally determined by measuring the scattering intensity of evanescent light. Without the particle, the light intensity has an exponential dependence on the distance z from the glass plate, $I(z) = I_0 e^{-\beta z}$, where β is a known quantity depending on refractive indices and the wavelength. When the particle is put at a distance h from the glass plate the scattered intensity is thus proportional to $e^{-\beta h}$, so that a temporal recording of the scattered intensity determines the probability of finding the particle at all distances. The potential $V_{total}(h)$ follows from these experimental raw data by inversion of the Boltzmann distribution.

Figure 3 shows the result of this procedure after subtracting $G_{eff}(h-a)$ for a 10 nm polystyrene sphere over silica for various electrolyte concentrations [6]. Since the distance dependence of $V(h)$ in eq. 18 is only in the exponential factor, whereas the prefactors γ_c and γ_w depend on κ , the different results in Fig. 3 must collapse onto a single master curve when $\beta V(h)/\gamma_c \gamma_w$ is plotted over $\kappa(h-a)$; this is indeed the case as shown in Fig. 4. Finally, it is worth mentioning that this procedure [6] provides a sensitive method to measure the colloid charge density $\sigma_c = Z/4\pi a^2$, since the prefactor γ_c , determined from the experiment, is related to σ_c by

$$\gamma_c = \tanh\left[\frac{1}{2} \operatorname{arcsinh}\left(2\pi\lambda_B \sigma_c / \kappa\right)\right]. \quad (20)$$

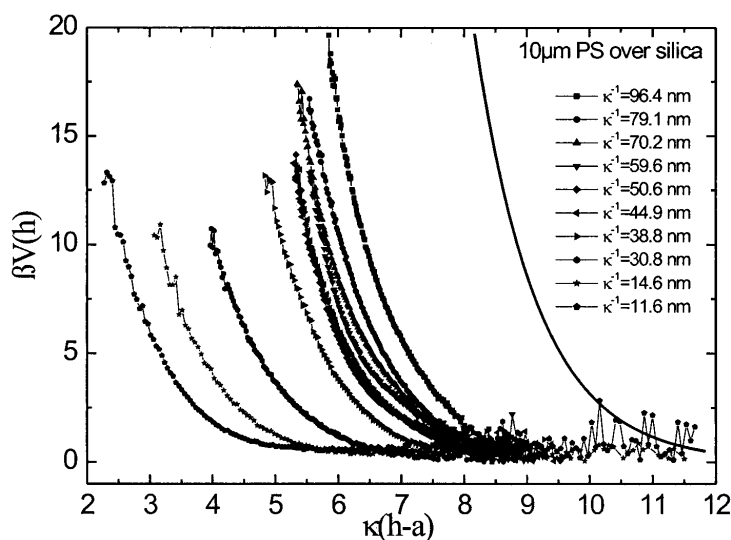


Fig. 3 Effective double-layer potentials between a glass surface and a colloidal sphere, experimentally determined for various salt concentrations using the TIRM method. The function $16ae^{-\kappa(h-a)}/\lambda_B$ is plotted as solid line. Taken from [6].

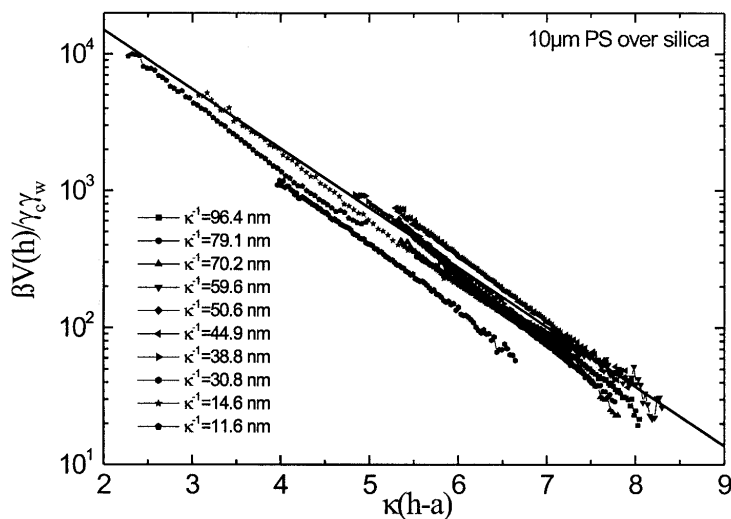


Fig. 4 The potentials of Fig. 3 divided by $\gamma_w \gamma_c$ all collapse onto the simple function $16ae^{-\kappa(h-a)}/\lambda_B$, appearing as a line in this logarithmic plot. Taken from [6].

CHARGED ROD INTERACTING WITH AN OPPOSITELY CHARGED PLANAR INTERFACE

Recent experiments have investigated DNA strands approaching a cationic lipid membrane [7]. DNA is a highly charged polyelectrolyte; the distance τ^{-1} (τ is the line charge density) between ionizable groups is so high that $l_B \tau \approx 4$. Therefore, a large number of counterions are condensed on the polymer when it

is far away from other charged objects in the bulk of an aqueous solvent [13]. It is natural in the present context to investigate a simple model that tries to cover the essential ingredients of the electrostatic problem of the effective interaction between the polyelectrolyte and the charged membrane.

DNA has a persistence length as high as 50 nm, so it is reasonable to model the DNA as a negatively charged and infinitely long, stiff rod of radius $r_0 = 1$ nm. The membrane, on the other hand, is modeled by a stiff and infinitely extended planar interface. The rod axis is parallel to the interface. In view of the experiments mentioned above, a cationic membrane is considered. Contrary to our previous case of a sphere in front of a wall, the interacting objects, rod, and interface, are now oppositely charged, and so are their respective counterions. When the distance h between rod and wall is large the positive counterions perfectly screen the negatively charged rod and the negative counterions screen the positively charged wall. With decreasing h the two ion clouds begin to overlap, and the resulting effects on the rod-wall interaction shall now be discussed [14,15].

The approach used to quantitatively calculate the effective interaction as a function of rod-wall distance h is similar in spirit to the one described above for the sphere-wall geometry [15]. The task is to determine the grand canonical potential $\Omega(h)$ like in eq. 5, where the dielectric constants ϵ' of the interface and the rod are assumed to be very small compared to ϵ of water. To calculate the electrostatic potential $\phi(\mathbf{r})$ and the ion distributions $\rho_{\pm}(\mathbf{r})$, needed to evaluate $\Omega(h)$, it is again necessary to solve the PB eq. 1 in the region outside the rod and the interface, but now with different boundary conditions. Equation 3 is replaced by

$$\mathbf{n}_c \cdot \nabla \phi(\mathbf{r}) = 2\lambda_B \tau / r_0 \quad (21)$$

for \mathbf{r} on the surface of the rod, whose outward normal unit vector is \mathbf{n}_c . The condition on the interface, replacing eq. 4, is

$$\mathbf{n}_w \cdot \nabla \phi(\mathbf{r}) = -4\pi\lambda_B \sigma_w \quad (22)$$

The numerical solution for $\phi(\mathbf{r})$ is obtained after introducing bi-cylindrical coordinates. From it, the grand canonical potential and other thermodynamic properties are calculated as a function of h . It is convenient to consider all quantities relative to the uncharged rod at the same distance h , for example, $\tilde{\Omega} = \Omega^\tau - \Omega^0$ and $\tilde{N} = N^\tau - N^0$, where the superscript τ refers to the charged rod and 0 to the uncharged one. Moreover, these quantities are given per unit length of the rod and hence in units of $d = 1/\tau$.

For the understanding of the physics of various contributions to the effective rod-wall interaction it is instructive to first consider the total number N of ions in the system, which follows from the solution $\phi(\mathbf{r})$ of the PB boundary value problem,

$$N = 2c_s \int d\mathbf{r} \cosh \phi(\mathbf{r}). \quad (23)$$

It should be remembered that the problem is formulated in the grand canonical ensemble so that the chemical potential μ_s is fixed, but not N . Figure 5 shows results for \tilde{N}/τ as a function of h for different values of the surface charge density on the interface. The latter is given in terms of $\lambda_B \zeta = 2\pi r_0 \lambda_B \sigma_w$, so that the surface charge density becomes directly comparable to the dimensionless line charge density $\lambda_B \tau = 4$ of the DNA rod.

It is seen that \tilde{N} is always negative and that it decreases as the rod approaches the interface, eventually increasing again as h becomes very small. The decrease of the number of ions in the neighborhood of the two charged objects is known as counterion release [16] (or evaporation). It arises from the fact that the two overlapping double layers of wall and rod have opposite sign of charge; they dissolve each other in the sense that they are no longer needed to screen the fixed charges on their respective object. When the oppositely charged objects rod and wall are sufficiently close to each other, the fixed charges on one object contribute to the screening of the fixed charges on the other one, so that some of the mobile ions become useless. Counterions bound to the polyelectrolyte, when it is far away from the interface, are now released and move to the bulk (reservoir). In the special situation considered here,

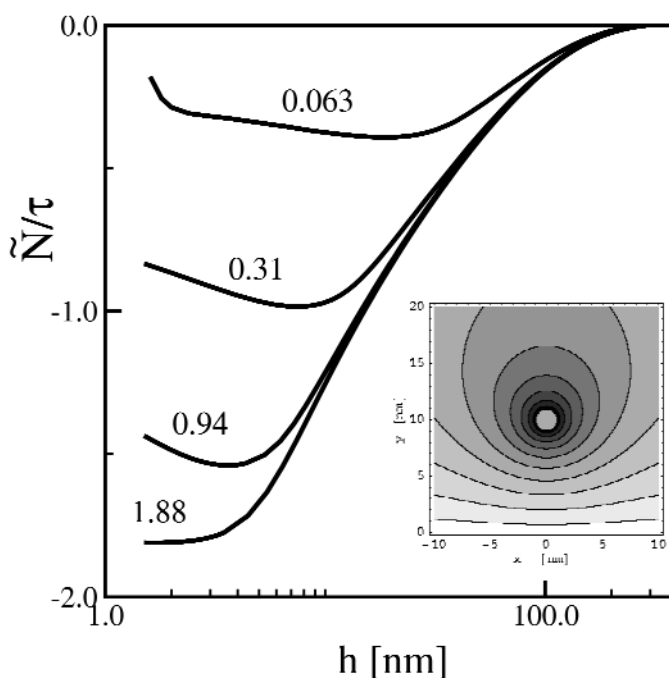


Fig. 5 The change \tilde{N} of the total number of screening mobile ions of the electrolyte as a function of the distance h between the negatively charged rod ($\lambda_B \tau = 4$) and the positively charged wall for different values of the wall charge density. The latter are given in units of $\lambda_B \zeta$ (labels at the curves). The electrolyte concentration corresponds to $\kappa^{-1} = 50$ nm. The inset shows the electrostatic potential ϕ for a rod-wall distance of 10 nm at a wall charge density corresponding to $\lambda_B \zeta = 0.94$. Taken from [15].

where the negatively charged polyelectrolyte approaches a positively charged interface, the Manning condition of counterion condensation is relaxed.

The increase of \tilde{N} as h becomes small is a result of image charge effects. The image charges of the fixed charges on the rod have the same polarity as the latter; they give thus rise to an effective repulsion. When at small values of h the image charges become more important than those sitting at the interface, the image charges have to be screened, and as a result \tilde{N} increases again with decreasing h . It is also intuitively evident that this effect is more important for smaller values of the wall-charge density $\lambda_B \zeta$ and that this effect extends to larger values of h in this case, see Fig. 5.

The release of counterions has a pronounced effect on the effective rod-wall interaction potential. In ref. 15, various contributions to the change of the grand potential $\tilde{\Omega}$ have been identified. There is always the attractive contribution $\tilde{\Omega}_w$ arising from the interaction of the bare charged rod in the unperturbed Gouy–Chapman layer. Starting from eq. 15, it is easy to obtain closed expressions for $\tilde{\Omega}_w$ in two limiting cases; for high electrolyte concentrations $\kappa \gg 2\pi l_B \sigma_w$ or large separations $h > \kappa^{-1}$

$$\beta \tilde{\Omega}_w \approx -\frac{4\pi l_B \tau \sigma_w}{\kappa} e^{-\kappa h} \quad (24)$$

and for small electrolyte concentrations and small distances

$$\beta \tilde{\Omega}_w \approx 2\tau \ln \frac{\kappa}{4\pi l_B \sigma_w} + 2\tau \ln(1 + 2\pi l_B \sigma_w h). \quad (25)$$

Writing $\tilde{\Omega} = \tilde{\Omega}_w + \Delta\tilde{\Omega}$, the remaining contributions consist of (i) repulsive image charge effects, (ii) repulsion due to the distortion of the ion clouds, and (iii) the attractive counterion release interaction. Whereas $\tilde{\Omega}_w$ is always negative, the results in Fig. 6 show that $\Delta\tilde{\Omega}$ can have either sign, depending on the parameter values. As seen from the behavior of \tilde{N} in Fig. 5, the counterion release effect becomes increasingly important as the surface charge density on the wall is increased, which reflects itself also in the formation of a minimum of $\Delta\tilde{\Omega}$ in Fig. 6. This minimum develops as a result of the competition between the repulsive image charge and ion cloud deformation effect at short distances and the longer-ranged attraction that is due to the counterion release. This minimum survives when the attractive part $\tilde{\Omega}_w$ is added, so that the effective rod-wall potential $\tilde{\Omega}(h)$ has a minimum at small but finite values of h for the electrolyte concentration corresponding to $\kappa^{-1} = 50$ nm, which was used for these calculations. Therefore, the rod should bind to the membrane at small but finite values of h . Since the addition of salt screens the wall-rod attraction, unbinding should result from an increase of electrolyte concentration.

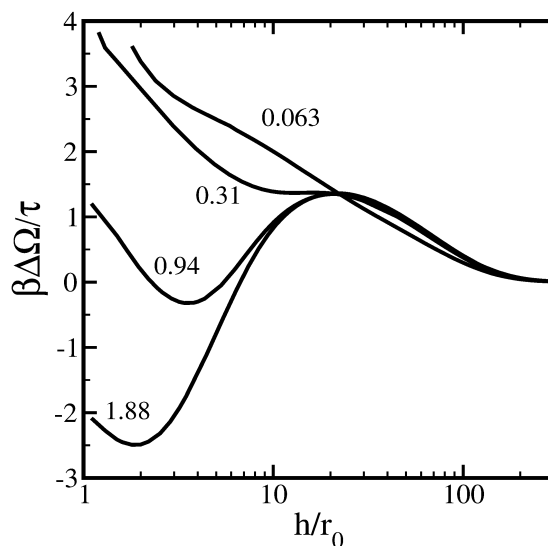


Fig. 6 The contribution $\beta\Delta\tilde{\Omega}$ of the total effective interaction $\beta\tilde{\Omega}$ as a function of distance h , scaled by the radius r_0 of the rod, for the same values of the wall charge density as in Fig. 5. Taken from [15].

Knowing the behavior of the grand canonical potential $\Omega(h)$, it is possible to calculate other thermodynamic functions. It is found that the counterion release gives rise to a loss of entropy; \tilde{S} decreases as h decreases, which is to be expected since a loss of particles, \tilde{N} , leads to a loss of entropy. The quantity which increases, as the counterion release mechanism becomes more important, is not the entropy, but the enthalpy

$$\beta\tilde{H} = \frac{5}{2}\tilde{N} + \frac{1}{k}\tilde{S}_p \quad (26)$$

where

$$\tilde{S}_p = \left(\frac{S^\tau}{N^\tau} - \frac{S^0}{N^0} \right) N^\tau \quad (27)$$

is the total entropy change of all those ions remaining in the system. And it is this quantity, which can be shown to be responsible for the counterion-release force [15].

For a more realistic model of a biomembrane, one has to take into account charge-regulation [17] and the mobility of ionizable and neutral lipids on the surface of the membrane. This leads to a more complicated boundary condition at the surface of the membrane. The surface charge density depends on a given pH value of the electrolyte solution, a given set of dissociation constants, and the position-dependent surface potential, which is in turn determined by the location of the charged rod [18]. These effects have then to be combined with the mobility of groups, so that they can move within the membrane, depending on the signs and magnitudes of their charges, in response to the location of charged objects approaching the membrane. The resulting surface charge density becomes a function of the electrostatic potential, so that the boundary condition depends on the solution of the PB equation. The appropriate boundary value condition has recently been derived, and it has been used to investigate the DNA adsorption behavior [18]. It is found that membrane fluidity can have considerable impact at short distances. It becomes possible that the negatively charged rod can bind to a globally negatively charged membrane, if the latter consists of more negative than positive charges; the positive charges can accumulate in a region, where the negatively charged rod approaches the membrane, so that they can bind the rod.

PHASE BEHAVIOR OF CHARGE-STABILIZED COLLOIDAL SUSPENSIONS

It is known since van der Waals that a one-component system can only phase-separate into a dilute and a dense liquid phase if there are attractive interactions between the constituents. The loss of entropy has to be overcompensated by a gain in internal energy in order for the free energy of the two coexisting phases to be smaller than the one of the homogeneous system. Since the DLVO interaction between charge-stabilized particles is inevitably repulsive, a naive expectation is that fluid–fluid coexistence cannot exist in suspensions of such particles. This view is, however, in contrast to observations of void structures in the bulk of suspensions of highly deionized suspensions [8].

A way out of this puzzle came with the recognition of further terms in the total potential energy beyond the sum of pair interactions [19]. The DLVO potential is a one-component description of a multicomponent system, and a more careful investigation shows that there are contributions to the total potential energy, which are independent of the particle positions but which depend on the colloid number density and other parameters in a nonlinear fashion [20]. These so-called volume terms were found to produce van der Waals-loops in the phase diagram such that the system at a salt concentration in the micro-molar regime can phase-separate into an extremely dilute (gas) phase and a denser liquid phase.

These predictions are based on approximations that are equivalent to the linearized PB equation. It is, therefore, desirable to use a different approach that avoids the linearization. A procedure, recently developed [21], which makes use of the nonlinear PB boundary value ideas described above for the colloid-interface problems, will now be summarized.

The starting point is the free energy A of N colloids in a volume V ,

$$\exp[-\beta A] = \frac{1}{N! \Lambda^{3N}} \int d\mathbf{R}^N \exp[-\beta \Omega(\mathbf{R}^N)], \quad (28)$$

where $\Omega(\mathbf{R}^N)$ is the many-body Hamiltonian of the one-component system of dressed colloids at positions $\mathbf{R}^N \equiv \{\mathbf{R}_1, \dots, \mathbf{R}_N\}$. This quantity is just the grand canonical potential of the three-component system of colloids, counter- and coions with the colloids being held fixed in the configuration \mathbf{R}^N . Therefore, $\Omega(\mathbf{R}^N)$ is given by an expression like in eq. 5 (without the second term), in which the region G of integration is the total volume V excluding the volumes occupied by the colloids. To evaluate the integrals in eq. 5 it is necessary to solve the PB eq. 1 for the electrostatic potential with the boundary condition (3) on each of the colloids sitting at the positions \mathbf{R}^N . In order to avoid this difficult task the cell model is introduced.

The cell model assumes that the integral in eq. 28, which is over all the configurations the N colloidal particles can take on, can be approximated by the most important configuration. Since the colloids repel each other strongly, they will mostly be in a configuration where they have the maximum distance from each other. Assuming a fcc-crystal configuration, eq. 28 becomes

$$A = N(f^{id} + f^{ex}), \quad (29)$$

where $\beta f^{id} = \log n_p \Lambda^3 - 1$ is the ideal-gas free energy per colloidal particle with $n_p = N/V$ being the colloid number density, and $f^{ex} = \Omega(\mathbf{R}_{fcc}^N)/N$ the excess free energy per colloidal particle. Since the crystal consists of identical Wigner–Seitz cells, it is now sufficient to solve the PB equation in only one cell. Assuming further that the cell can be approximated by a sphere of radius R , the PB equation becomes a one-dimensional nonlinear equation with the boundary condition of eq. 3 at $r = a$. At the boundary of each cell the electric fields have to vanish, so that $\nabla\phi = 0$ at $r = R$. It is important to notice that the electrostatic potential and therefore Ω and A depend on the density of colloids through R , since the volume of the cell is given by $V_m = 4\pi R^3/3 = 1/n_p$.

Using expression (6) for Ω without the first term, one obtains immediately

$$\beta f^{ex} = -\frac{Z}{2} \left(\phi(a) - \frac{Z\lambda_B}{a} \right) + 4\pi c_s \int_a^R dr r^2 [\phi(r) \sinh \phi(r) - 2 \cosh \phi(r) + 2], \quad (30)$$

which can be evaluated with the numerical solution of the one-dimensional nonlinear PB equation.

In order to clarify the relation of this cell-model approach to the volume-term theory proposed by van Roij *et al.* [20], the PB equation and the expression (30) for the excess free energy are linearized about a finite value $\bar{\phi}$ of the electrostatic potential $\phi(r)$. Using for $\bar{\phi}$ the average of $\phi(r)$ over the region of the cell outside the colloidal sphere, which is known as the Donnan potential,

$$4\pi \int_a^r dr r^2 [\phi(r) - \bar{\phi}] = 0, \quad (31)$$

and inserting into this definition the analytic solution of the PB equation, linearized about $\bar{\phi}$, the closed expression

$$\sinh \bar{\phi} = \frac{\eta}{\eta - 1} \frac{3Z}{8\pi c_s a^3} \quad (32)$$

is obtained, which shows that $\bar{\phi}$ depends on the volume-fraction $\eta = 4\pi a^3 n_p / 3$ of the colloids.

This value of $\bar{\phi}$ is then used in an expansion of eq. 30, from which a closed expression for an approximation βf_{Don}^{ex} to βf^{ex} is obtained. This expression reduces to the Debye–Hückel limiting law as $\eta \rightarrow 0$. The result for βf_{Don}^{ex} depends in a nonlinear fashion on the salt concentration c_s and the volume-fraction η of the colloids, and it is nearly identical to the volume terms obtained in [20], thus identifying the approach by van Roij *et al.* as a PB theory with the PB equation being linearized about the Donnan potential.

It is now possible to compare the predictions based on the cell model and the nonlinear solution of the PB equation, eq. 30, with those based on βf_{Don}^{ex} . In order to investigate the existence of a spinodal instability and a corresponding gas–liquid coexistence, it is necessary to calculate the isothermal compressibility $\partial p / \partial n_p$ with p the osmotic pressure of the suspension given by $p = n_p^2 (\partial f / \partial n_p)$. Figure 7 shows the results for three values of the number of charges Z per colloid. While the Donnan approximation leads to negative values of the compressibility and therefore to an instability with respect to phase separation for $Z = 3500$, the cell model with the nonlinear PB solution does not give rise to such an instability. Such calculations have been performed for many combinations of the parameters Z , c_s , and η , but no instability has been found on the basis of the nonlinear cell model [21].

Closer inspection of the problem shows that the free energy at zero volume-fraction—the self-energy—is of considerable importance in our context. The difference between βf_{Don}^{ex} and βf^{ex} at $\eta = 0$, i.e., between the self-energy in linearized and in nonlinear theory, increases with increasing Z . This can

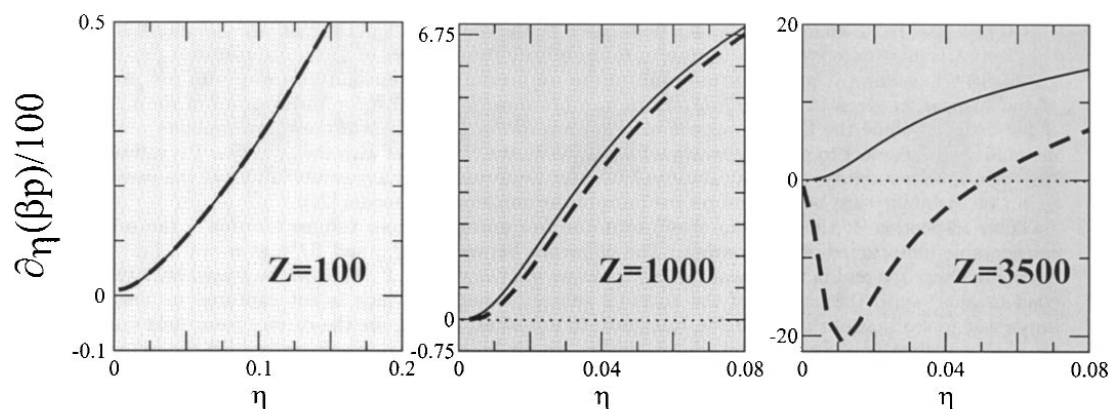


Fig. 7 The compressibility of a colloidal suspension as a function of the colloid packing fraction η for colloidal charges $Z = 100$, 1000 , and 3500 . The full lines are based on the solution of the nonlinear PB cell model while the dashed lines result when the PB equation is linearized about the Donnan potential. A perfect agreement at $Z = 100$ develops into a dramatic mismatch at high Z , indicating a spinodal instability in linear, but not in nonlinear theory. Taken from [21].

be traced back to the “counterion condensation” onto the surface of the colloidal sphere, something that is not captured by linear theory. It is important to see that our self-energies, calculated in nonlinear theory, are the correct mean-field self-energies. They are not dependent on the cell model approximation, simply because at zero volume-fraction the cell is infinitely large. It can thus be ruled out that the difference between linear and nonlinear theory at $\eta = 0$ stems from the cell model: It comes from nothing but the linearization. It might be that the cell model approximation fails at low, but finite volume-fraction; at high volume-fraction, however, we can expect it to be a reliable approximation. Taken together, we have reliable nonlinear information about the free energies at high volume-fraction and at $\eta = 0$. But it is only these two elements that are really needed to prove that the Donnan linearization, i.e., the volume-term theory, produces unphysical results.

It has to be emphasized that the cell model is an approximation that becomes less realistic and less reliable at low volume-fractions. Thus, our present approach is certainly not adequate to rule out the possible existence of a fluid–fluid phase coexistence at low volume-fraction in general. It is, however, good enough to demonstrate that the fluid–fluid coexistence predicted in [20]—which is based on a theory that requires further approximations and is thus even simpler than ours—arises from a failure of the linearization. In summary, one may thus conclude that the phase behavior of charge-stabilized colloidal suspensions is still far from being understood, in particular at low volume-fraction and in highly deionized suspensions.

CONCLUDING REMARKS

The main aim of this contribution has been to investigate for several realistic examples the consequences of the high accumulation of the ion distributions in the immediate neighborhood of charged objects in electrolyte solutions. The strong variations of these distributions are only captured by the nonlinear PB equation and are not adequately described by linear theories. The disadvantage is that no analytic expressions exist for the solutions of the nonlinear equation for most cases and that the superposition principle can no longer be used. Under some circumstances, such as for the case of the spherical particle close to a flat interface, it is possible to justify certain closed expressions for approximate effective interaction potentials by testing them against the exact numerical solution. As a result, parameter ranges can be identified, in which the approximate expressions are useful.

There are other cases, however, where qualitatively different predictions are obtained, when the full nonlinear problem is solved. An example of this kind is the phase behavior of charge-stabilized suspensions: The coexistence of a dilute, gas-like phase with a dense, fluid-like phase, which is obtained in the linearized version of the cell model, disappears in nonlinear theory.

ACKNOWLEDGMENTS

The authors are grateful for several helpful discussions with R. Netz and R. van Roij. The work by C. Fleck, G. Klein, and E. C. Mbamala on the subject of this contribution is very much appreciated. The financial support by the Deutsche Forschungsgemeinschaft (SFB 513) is acknowledged.

REFERENCES

1. J.-P. Hansen and H. Löwen. *Annu. Rev. Phys. Chem.* **51**, 209 (2000).
2. C. N. Likos. *Physics Reports* **348**, 267 (2001).
3. E. J. W. Verwey and J. T. G. Overbeek. *Theory of the Stability of Lyophobic Colloids*, Elsevier, Amsterdam (1948).
4. L. Guldbrand, B. Jönsson, H. Wennerström, P. Linse. *J. Chem. Phys.* **80**, 2221 (1984).
5. H. Greberg, R. Kjellander, T. Akesson. *Mol. Phys.* **92**, 35 (1997); H. Greberg and R. Kjellander. *J. Chem. Phys.* **108**, 2940 (1998); M. J. Stephens and M. O. Robbins. *Europhys. Lett.* **12**, 81 (1990); Z. Tang, L. E. Scriven, H. T. Davis. *J. Chem. Phys.* **97**, 9258 (1992); P. Linse and V. Lobaskin. *J. Chem. Phys.* **112**, 3917 (2000).
6. H. H. von Grünberg, L. Helden, P. Leiderer, C. Bechinger. *J. Chem. Phys.* **114**, 10094 (2001).
7. J. O. Rädler, I. Koltover, T. Salditt, C. R. Safinya. *Science* **275**, 810 (1997), T. Salditt, I. Koltover, J. Rädler, C. R. Safinya. *Phys. Rev. Lett.* **79**, 2582 (1997); B. Maier and J. O. Rädler. *Phys. Rev. Lett.* **82**, 1911 (1999).
8. B. V. R. Tata, E. Yamahara, P. V. Rajamani, N. Ise. *Phys. Rev. Lett.* **78**, 2660 (1997); H. Yoshida, J. Yamanaka, T. Koda, N. Ise, T. Hashimoto. *Langmuir* **14**, 569 (1998).
9. H. H. von Grünberg and E. C. Mbamala. *J. Phys.: Condens. Matter* **13**, 4801 (2001).
10. F. H. Stillinger. *J. Chem. Phys.* **35**, 1584 (1961).
11. D. F. Evans and H. Wennerström. *The Colloidal Domain: Where Physics, Chemistry, Biology and Technology Meet*, VCH, New York (1994).
12. See J. Y. Walz. *Curr. Opin. Colloid Interface Sci.* **2**, 600 (1997) for a recent review.
13. G. S. Manning. *J. Chem. Phys.* **51**, 954 (1969).
14. P. Sens and J. F. Joanny. *Phys. Rev. Lett.* **84**, 4862 (2000).
15. C. Fleck and H. H. von Grünberg. *Phys. Rev. E* **63**, 061804 (2001).
16. V. A. Parsegian and D. Gingell. *Biophys. J.* **2**, 1192 (1972); P. L. de Haseth, T. M. Lohman, M. T. Record. *Biochemistry* **16**, 4783 (1977).
17. B. Ninham and V. A. Parsegian. *J. Theor. Biol.* **31**, 405 (1971).
18. C. Fleck, R. R. Netz, H. H. von Grünberg. *Biophys. J.* **82**, 76 (2001).
19. M. J. Grimson and M. Silbert. *Mol. Phys.* **74**, 397 (1991).
20. R. van Roij and J. P. Hansen. *Phys. Rev. Lett.* **79**, 3082 (1997); R. van Roij, M. Dijkstra, J. P. Hansen. *Phys. Rev. E* **59**, 2010 (1999).
21. H. H. von Grünberg, R. van Roij, G. Klein. *Europhys. Lett.* **55**, 580 (2001).